Available online at www.sciencedirect.com
SCIENCE DIRECT®
Computers and Structures 83 (2005) 2121–2136
Computers & Structures
www.elsevier.com/locate/compstruc

A comparative study of metamodeling methods for multiobjective crashworthiness optimization

H. Fang [a,*], M. Rais-Rohani [b], Z. Liu [c], M.F. Horstemeyer [a,d]

[a] Center for Advanced Vehicular Systems, Mississippi State University, Mississippi State, MS 39762, USA
[b] Department of Aerospace Engineering, Mississippi State University, Mississippi State, MS 39762, USA
[c] Department of Civil Engineering, Mississippi State University, Mississippi State, MS 39762, USA
[d] Department of Mechanical Engineering, Mississippi State University, Mississippi State, MS 39762, USA

Received 28 January 2004; accepted 28 February 2005
Available online 24 June 2005

Abstract

The response surface methodology (RSM), which typically uses quadratic polynomials, is predominantly used for metamodeling in crashworthiness optimization because of the high computational cost of vehicle crash simulations. Research shows, however, that RSM may not be suitable for modeling highly nonlinear responses that can often be found in impact related problems, especially when using limited quantity of response samples. The radial basis functions (RBF) have been shown to be promising for highly nonlinear problems, but no application to crashworthiness problems has been found in the literature. In this study, metamodels by RSM and RBF are used for multiobjective optimization of a vehicle body in frontal collision, with validations by finite element simulations using the full-scale vehicle model. The results show that RSM is able to produce good approximation models for energy absorption, and the model appropriateness can be well predicted by ANOVA. However, in the case of peak acceleration, RBF is found to generate better models than RSM based on the same number of response samples, with the multiquadric function identified to be the most stable RBF. Although RBF models are computationally more expensive, the optimization results of RBF models are found to be more accurate.

Keywords: Metamodeling; Crashworthiness; Multiobjective optimization; Radial basis function; Response surface methodology

1. Introduction

In 2002, 42,815 people were killed in vehicle crashes. That represents an increase of 1.5% over 2001 and the highest level since 1990 [1]. Also in 2002, 2,926,000 people were injured from vehicle crashes, many with permanent injuries. In recent years, vehicle safety (crashworthiness) has drawn more public attention and research on vehicle crashworthiness has gained momentum in both academe and the automotive industry.

Vehicle safety can be measured by parameters such as the contact forces exerted on the occupants and/or the resulting accelerations during a vehicle crash [2]. Both safety parameters (i.e., contact force and acceleration) are closely related to the amount of energy absorbed by the vehicle before the impact wave reaches the occupants. With the aid of finite element (FE) analysis

* Corresponding author. Tel.: +1 662 325 6696; fax: +1 662 325 5433.
E-mail address: hfang@cavs.msstate.edu (H. Fang).

0045-7949/$ - see front matter © 2005 Elsevier Ltd. All rights reserved.
doi:10.1016/j.compstruc.2005.02.025

programs designed for dynamic contact problems, such as LS-DYNA and PAM-CRASH, it is possible to perform a crash simulation and evaluate these parameters. Furthermore, by coupling such simulation tools with nonlinear mathematical programming procedures, we can optimize a vehicle body to improve its crashworthiness characteristics while considering other important factors such as manufacturing cost and vehicle performance. However, there are many challenges with crashworthiness optimization. Among them, we can point to the implicit relationships between safety parameters and structural design attributes as well as the computational cost associated with repeated transient FE analyses. Such concerns have led to the widespread use of metamodeling approaches in crashworthiness optimization.

Despite their efficiency, metamodeling techniques could still require a significant number of crash simulations, especially when the number of design variables is large. For this reason, reduced models (i.e., component FE models or full-vehicle FE models with fewer degrees of freedom) have been developed and used in crash simulations [3–6]. Although helpful in understanding the mechanism of crash and improving vehicle designs, the reduced models have two major limitations. Firstly, it is difficult to accurately match the exact structural constraint and loading conditions in the reduced model with those in a full-scale model during impact accompanied with large deformations. Secondly, a reduced model can typically be used for only one impact scenario and as such it would not be appropriate for crashworthiness optimization involving multiple impacts. However, the recent advances in computer technology have made it possible to use full-scale FE models in high fidelity crash simulations. Such models, developed by the National Crash Analysis Center (NCAC) and other agencies in the US, have been successfully used for crash simulation with the results compared with real vehicle tests [7–10].

Among the commonly used metamodeling techniques in crashworthiness optimization, the response surface methodology (RSM), particularly the use of second-order polynomials, has been the predominant method mainly because of its simplicity and efficiency. However, the drawback of using second-order response surface (RS) models is that they may not be appropriate for creating global models over the entire design space for highly nonlinear problems. Although it is possible to develop higher-order RS models, they may not be effective or appropriate for crashworthiness optimization, partly due to the high computational cost in extensive sampling of the design space.

Recent innovations to improve both the accuracy and efficiency of RSM include the development and application of the sequential local RSM [11,12], adaptive RSM [13], and trust-region-based RSM [14]. All these approaches partition the feasible design space into multiple small regions that can be accurately represented by low-order RS models. Although these techniques are very efficient for single objective optimization problems, they may not be appropriate for problems involving multiple objectives. Yang et al. [15], in their survey of literature on local RSM approaches, have concluded that in multiobjective optimization problems these approaches could be ineffective because the response region of interest would never be reduced to a small neighborhood that was good for all the objectives that typically conflict with each other.

Jin et al. [16], compared RSM, Kriging method (KM), radial basis functions (RBF), and multivariate adaptive regression splines (MARS) using fourteen different problems, with one representing a complex engineering application. They showed that RBF was the best for both large-scale and small-scale problems based on evaluations of the coefficient of multiple determination (R^2), relative average absolute error (RAAE), and relative maximum absolute error (RMAE). RBF was found to be the best for overall performance on accuracy, robustness, problem types, sample size, efficiency, and simplicity. By contrast, they showed RSM to be the worst, in fact not suitable, for modeling highly nonlinear problems. However, they used only a linear RBF that, in general, is not a very accurate metamodel for modeling highly nonlinear problems. Krishnamurthy [17] compared augmented and compactly supported RBF with KM, local moving least square (MLS), and global least square (GLS) using one mathematical function and one FE based problem. The MLS and GLS models in his study were basically quadratic polynomials; therefore, they represented local and global RS models, respectively. He showed that RBF, KM, and MLS produced comparable and accurate results, and that GLS performed poorly. However, the example problems in that study did not require complex engineering analysis and thus relatively large sample sizes were generated and used.

Despite its simplicity, RSM provides efficient yet accurate solutions to many engineering problems [18] and analysis of variance (ANOVA) can be used to predict model appropriateness or fitness before the model is used in design optimization. RBF, on the other hand, is more expensive than RSM, because it uses a series of computationally expensive functions for a single model; therefore, it is less efficient in performing function evaluations. This drawback becomes apparent when solving multiobjective design optimization problems in which millions sometimes even billions of solutions need to be found in order to develop the Pareto Frontier. Another disadvantage of using RBF is that model fitness cannot be checked using ANOVA, because by definition an RBF passes exactly through all the design points.

The focus of this study is to compare RSM and RBF using limited samplings from both a nonlinear mathe-

matical function and full-scale crash simulations, and to assess the appropriateness of the resulting metamodels in both problems. The remaining portion of the paper is organized as follows. In Section 2 a brief overview of RSM and RBF is provided followed by the metamodeling of a nonlinear mathematical function in Section 3. In Section 4, we describe the crash simulation model, multiobjective optimization problem, and corresponding results. This is followed by the concluding remarks in Section 5.

2. Metamodeling methodologies

The basic idea of metamodeling is to construct an approximate model using function values at some sampling points, which are typically determined using experimental design methods such as factorial design, Latin hypercube, central composite design, or Taguchi orthogonal array. Model fitness is subsequently checked using various statistical methods. In this section, we give a brief overview of the two methods of interest in our research.

2.1. Response surface methodology (RSM)

In RSM, we typically use first- or second-order models in the form of linear or quadratic polynomial functions to develop an approximate model that provides an explicit relationship between design variables and the response of interest. The unknown coefficients in the model are approximated using the method of least squares.

Let $f(\boldsymbol{x})$ be the true objective or response function and $f'(\boldsymbol{x})$ its approximation obtained using the second-order polynomial in the form

$$f'(\boldsymbol{x}) = \beta_0 + \sum_{i=1}^{m} \beta_i x_i + \sum_{i=1}^{m} \beta_{ii} x_i^2 + \sum_{i=1}^{m-1} \sum_{j=i+1}^{m} \beta_{ij} x_i x_j, \quad (1)$$

where m is the total number of design variables, x_i is the ith design variable, and the βs are the unknown coefficients. For n sampling of design variables $x_{ki}(k = 1,2 \ldots n, i = 1,2,\ldots m)$ and the corresponding function values $f_k(k = 1,2 \ldots n)$, Eq. (1) leads to n linear equations expressed as

$$\begin{aligned} f_1 &= \hat{\beta}_0 + \sum_{i=1}^{m} \hat{\beta}_i x_{1i} + \sum_{i=1}^{m} \hat{\beta}_{ii} x_{1i}^2 + \sum_{i=1}^{m-1} \sum_{j=i+1}^{m} \hat{\beta}_{ij} x_{1i} x_{1j}, \\ f_2 &= \hat{\beta}_0 + \sum_{i=1}^{m} \hat{\beta}_i x_{2i} + \sum_{i=1}^{m} \hat{\beta}_{ii} x_{2i}^2 + \sum_{i=1}^{m-1} \sum_{j=i+1}^{m} \hat{\beta}_{ij} x_{2i} x_{2j}, \\ &\cdots \\ f_n &= \hat{\beta}_0 + \sum_{i=1}^{m} \hat{\beta}_i x_{ni} + \sum_{i=1}^{m} \hat{\beta}_{ii} x_{ni}^2 + \sum_{i=1}^{m-1} \sum_{j=i+1}^{m} \hat{\beta}_{ij} x_{ni} x_{nj}. \end{aligned} \quad (2)$$

Eq. (2) may be expressed in matrix form as

$$\boldsymbol{f} = \boldsymbol{X}\hat{\boldsymbol{\beta}}, \quad (3)$$

where the vector of unknown coefficients $\hat{\boldsymbol{\beta}}$ represents the least-square estimator of the true coefficient vector and is solved using the method of least squares as

$$\hat{\boldsymbol{\beta}} = (\boldsymbol{X}^{\mathrm{T}}\boldsymbol{X})^{-1}(\boldsymbol{X}^{\mathrm{T}}\boldsymbol{f}). \quad (4)$$

Statistical analysis techniques such as ANOVA can be used to check the fitness of an RS model and to identify the main effects of design variables. However, main effect analysis is not the focus of this study and will not be discussed here. The major statistical parameters used for evaluating model fitness are the F statistic, R^2, adjusted $R^2(R^2_{\mathrm{adj}})$, and root mean square error (RMSE). Note that these parameters are not totally independent of each other and are calculated as

$$F = \frac{(\mathrm{SST} - \mathrm{SSE})/p}{\mathrm{SSE}/(n-p-1)}, \quad (5)$$

$$R^2 = 1 - \mathrm{SSE}/\mathrm{SST}, \quad (6)$$

$$R^2_{\mathrm{adj}} = 1 - (1-R^2)\frac{n-1}{n-p-1}, \quad (7)$$

$$\mathrm{RMSE} = \sqrt{\frac{\mathrm{SSE}}{n-p-1}}, \quad (8)$$

where p is the number of non-constant terms in the RS model, SSE is the sum of square errors, and SST is the total sum of squares. SSE and SST are calculated as

$$\mathrm{SSE} = \sum_{i=1}^{n} (f_i - f_i')^2, \quad (9)$$

$$\mathrm{SST} = \sum_{i=1}^{n} (f_i - \bar{f})^2, \quad (10)$$

where f_i is the measured function value at the ith design point, f_i' is the function value calculated from the polynomial at the ith design point, and $\bar{f}$ is the mean value of f_i.

Generally speaking, the larger the values of R^2 and R^2_{adj}, and the smaller the value of RMSE, the better the fit. In situations where the number of design variables is large, it is more appropriate to look at R^2_{adj}, because R^2 always increases as the number of terms in the model is increased while R^2_{adj} actually decreases if unnecessary terms are added to the model [19]. In addition to these statistics, the accuracy of the RS model can also be measured by checking its predictability of response using the prediction error sum of squares (PRESS) and R^2 for prediction ($R^2_{\mathrm{prediction}}$). The PRESS statistic and $R^2_{\mathrm{prediction}}$ are calculated as

$$\mathrm{PRESS} = \sum_{i=1}^{n} [f_i - f'_{(i)}]^2, \quad (11)$$

$$R^2_{\text{prediction}} = 1 - \text{PRESS}/\text{SST}, \tag{12}$$

where $f'_{(i)}$ is the predicted value at the ith design point using the model created by $(n-1)$ design points that exclude the ith point.

2.2. Radial basis functions (RBF)

An RBF uses a series of basic functions that are symmetric and centered at each sampling point, and it was originally developed for scattered multivariate data interpolation [20]. Applications of RBF include ocean depth measurement, altitude measurement, rainfall interpolation, surveying, mapping, geographics and geology, image warping, and medical imaging.

Let $f(\boldsymbol{x})$ be the true objective or response function and $f'(\boldsymbol{x})$ its approximation obtained from a classical RBF with the general form

$$f'(\boldsymbol{x}) = \sum_{i=1}^{n} \lambda_i \phi(\|\boldsymbol{x} - \boldsymbol{x}_i\|), \tag{13}$$

where n is the number of sampling points, $\boldsymbol{x}$ is the vector of design variables, $\boldsymbol{x}_i$ is the vector of design variables at the ith sampling point, $\|\boldsymbol{x} - \boldsymbol{x}_i\|$ is the Euclidean distance, ϕ is a basis function, and λ_i is the unknown weighting coefficient. Therefore, an RBF is actually a linear combination of n basis functions with weighted coefficients. Some of the most commonly used basis functions include:

- Thin-plate spline: $\phi(r) = r^2 \log(cr^2)$, $0 < c \leqslant 1$;
- Gaussian: $\phi(r) = e^{-cr^2}$, $0 < c \leqslant 1$;
- Multiquadric: $\phi(r) = \sqrt{r^2 + c^2}$, $0 < c \leqslant 1$;
- Inverse multiquadric: $\phi(r) = \frac{1}{r^2 + c^2}$, $0 < c \leqslant 1$.

By replacing $\boldsymbol{x}$ and $f'(\boldsymbol{x})$ in Eq. (13) with n vectors of design variables and their corresponding function values at the sampling points, we obtain the following n equations

$$\begin{aligned} f'(\boldsymbol{x}_1) &= \sum_{i=1}^{n} \lambda_i \phi(\|\boldsymbol{x}_1 - \boldsymbol{x}_i\|), \\ f'(\boldsymbol{x}_2) &= \sum_{i=1}^{n} \lambda_i \phi(\|\boldsymbol{x}_2 - \boldsymbol{x}_i\|), \\ &\cdots \\ f'(\boldsymbol{x}_n) &= \sum_{i=1}^{n} \lambda_i \phi(\|\boldsymbol{x}_n - \boldsymbol{x}_i\|). \end{aligned} \tag{14}$$

The matrix format of Eq. (14) is

$$\boldsymbol{f} = \boldsymbol{A}\boldsymbol{\lambda}, \tag{15}$$

where $\boldsymbol{f} = [f'(\boldsymbol{x}_1) f'(\boldsymbol{x}_2), \ldots, f'(\boldsymbol{x}_n)]^{\mathrm{T}}$, $A_{i,j} = \phi(\|\boldsymbol{x}_i - \boldsymbol{x}_j\|)$ $(i = 1, 2 \ldots n,\ j = 1, 2, \ldots n)$, and $\lambda = [\lambda_1 \lambda_2 \cdots \lambda_n]^{\mathrm{T}}$. The coefficient vector λ is obtained by solving Eq. (15).

An RBF using the aforementioned highly nonlinear functions does not work well for linear responses [17]. To solve this problem, we can augment an RBF by including a polynomial function such that

$$f'(\boldsymbol{x}) = \sum_{i=1}^{n} \lambda_i \phi(\|\boldsymbol{x} - \boldsymbol{x}_i\|) + \sum_{j=1}^{m} c_j p_j(\boldsymbol{x}), \tag{16}$$

where m is the total number of terms in the polynomial, and $c_j (j = 1, 2, \ldots, m)$ is the corresponding coefficient. A detailed discussion on the polynomial functions that may be used can be found in Ref. [17].

It can be seen that Eq. (16) is underdetermined because there are more parameters to be solved than the number of equations created with available sampling points. Therefore, the orthogonality condition is further imposed on coefficients λ as

$$\sum_{i=1}^{n} \lambda_i p_j(x_i) = 0, \quad \text{for } j = 1, 2 \ldots m. \tag{17}$$

Combining Eqs. (16) and (17) in matrix form gives

$$\begin{bmatrix} \boldsymbol{A} & \boldsymbol{P} \\ \boldsymbol{P}^{\mathrm{T}} & \boldsymbol{0} \end{bmatrix} \begin{bmatrix} \boldsymbol{\lambda} \\ \boldsymbol{c} \end{bmatrix} = \begin{bmatrix} \boldsymbol{f} \\ \boldsymbol{0} \end{bmatrix}, \tag{18}$$

where $A_{i,j} = \phi(\|\boldsymbol{x}_i - \boldsymbol{x}_j\|)$ $(i = 1, 2 \ldots n, j = 1, 2, \ldots n)$, $P_{i,j} = p_j(\boldsymbol{x}_i)$ $(i = 1, 2, \ldots n,\ j = 1, 2 \ldots m)$, $\lambda = [\lambda_1 \lambda_2 \ldots \lambda_n]^{\mathrm{T}}$, $\boldsymbol{c} = [c_1 c_2 \cdots c_m]^{\mathrm{T}}$ and $\boldsymbol{f} = [f'(\boldsymbol{x}_1) f'(\boldsymbol{x}_2) \cdots f'(\boldsymbol{x}_n)]^{\mathrm{T}}$. Eq. (18) consists of $(n + m)$ equations and its solution gives coefficients λ and $\boldsymbol{c}$ for the RBF in the form of Eq. (16).

It should be noted that an RBF passes through all the sampling points exactly. This means that function values from the approximate function are equal to the true function values at the sampling points. This can be seen from the way that the coefficients are found in Eq. (18). Therefore, it would not be possible to check RBF model fitness with ANOVA, which is a drawback of RBF.

3. Metamodeling with the branin rcos function

We start comparing the RS and RBF models with a highly nonlinear mathematical function, the Branin rcos function [21]. This function has two design variables and is given by

$$f(\boldsymbol{x}) = \left(x_2 - \frac{5 \cdot 1 x_1^2}{4\pi^2} + \frac{5 x_1}{\pi} - 6 \right)^2 + 10 \left(1 - \frac{1}{8\pi} \right) \cos(x_1) + 10, \tag{19}$$

where x_1 has a range of $[-5, 10]$ and x_2 has a range of $[0, 15]$.

We used a two-variable, seven-level full factorial design in sampling, which resulted in 49 (7^2 or 7×7) evenly distributed design points. We first created the linear and quadratic RS models with the 49 design points and

Table 1
Statistics of the RS models for the Branin rcos function on design points

RS model	F	$Pr > F$	R^2	R^2_{adj}	RMSE	PRESS	$R^2_{prediction}$
Linear polynomial	1.7	0.19	0.07	0.03	67.5	250249	0.0
Quadratic polynomial	19.8	<0.0001	0.70	0.66	39.8	101841	0.55

assessed their accuracies using Eqs. (5)–(12); the model statistics are given in Table 1. The small values of R^2, R^2_{adj}, and $R^2_{prediction}$ as well as the large values of RMSE and PRESS indicate bad fits of the two RS models, even though the quadratic model is better than the linear one. Using the same design samples, we also created the RBF models with the Gaussian, multiquadric, and inverse-multiquadric functions in both regular and augmented formats. The values of constant c in these basis functions were chosen to be one, and linear polynomials were used in the augmented RBF models. The Branin rcos function together with the RS and RBF models are illustrated in Fig. 1.

In Fig. 1, the symbols "RSM-LP" and "RSM-QP" stand for the RS models created with linear and quadratic polynomials, respectively. The RBF models created with the Gaussian, multiquadric, and inverse multiquadric functions are represented by symbols "RBF-GS", "RBF-MQ", and "RBF-IMQ", respectively. The augmented RBF models are represented by adding "-LP" to the symbols of those without augmentation. We can see from Fig. 1 that the two RS models

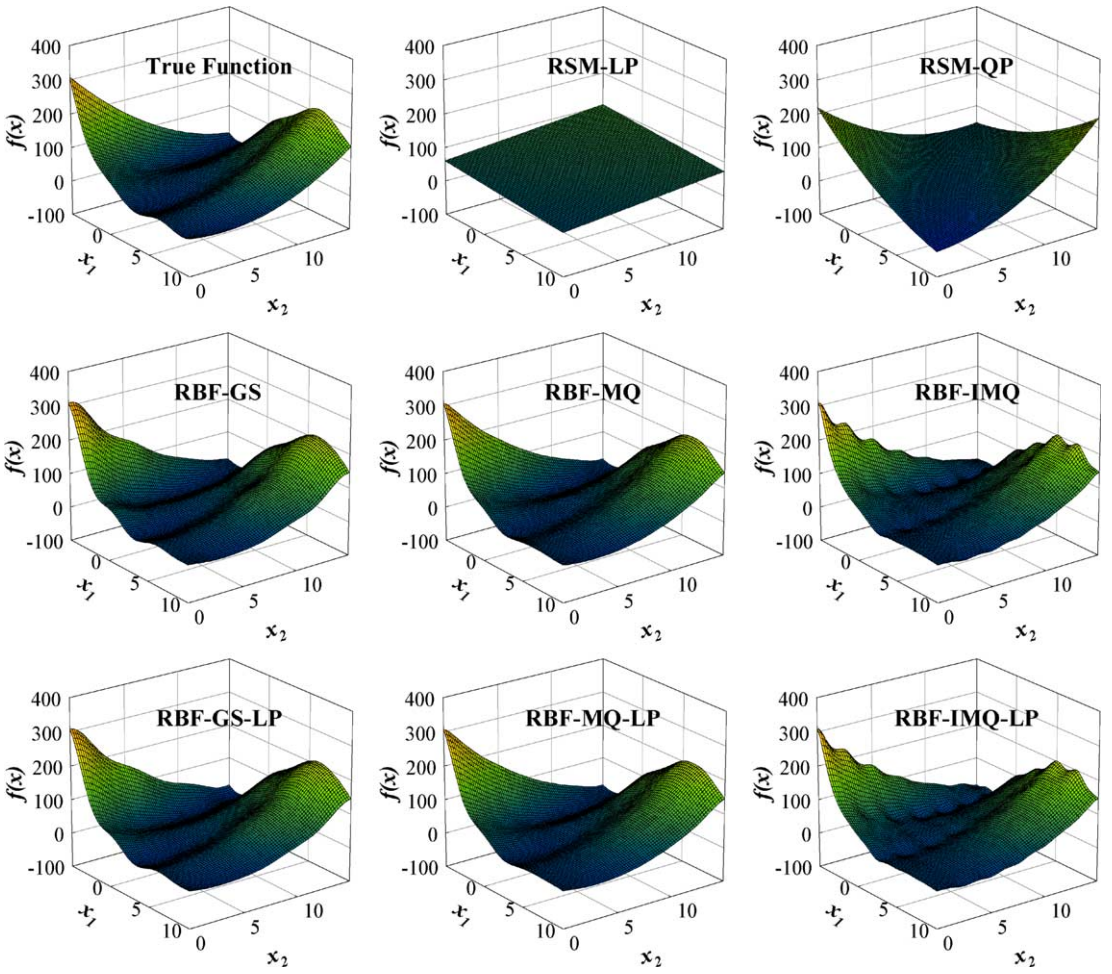

Fig. 1. The Branin rcos function and the metamodels.

Table 2
Accuracy assessment of the RS and RBF models for the Branin rcos function

Error	Metamodel							
	RSM-LP	RSM-QP	RBF-GS	RBF-MQ	RBF-IMQ	RBF-GS-LP	RBF-MQ-LP	RBF-IMQ-LP
Max. (%)	22247	10391	1321	1102	2676	666	1252	2937
Min. (%)	−79.7	−3596	−373	−37.3	−22.3	−478.6	−37.3	−19.7
RMSE	51.8	30.2	8.2	4.6	7.1	6.1	4.8	7.5

do not fit the true function well; this is consistent with the results of statistical assessment in Table 1. We also observed that all the RBF models have better fit than the RS models, with the two RBF models created with the multiquadric functions in regular and augmented format appearing to have the best fit.

As aforementioned, the model accuracy of an RBF model cannot be assessed on design points; therefore, we compared the accuracies of RS and RBF models at off-design points. We used points on a 76×76 grid and excluded the 49 design points in our evaluation; this resulted in a total of 5727 (5776–49) off-design points. The maximum errors, minimum errors, and RMSE values for all the metamodels were calculated; the results are given in Table 2. Comparing the absolute values of maximum and minimum errors and the RMSE values of the metamodels in Table 2, we found that all the RBF models predicted better than the RS models. The two RBF models created with the multiquadric function were identified to be the best.

4. Crashworthiness optimization problem

4.1. Finite element model

Our crashworthiness optimization problem is based on a full-scale FE model of 1996 Dodge Neon. The original FE model of this vehicle was developed by NCAC. It consists of 20 types of materials and 327 parts for a total mass of 1210 kg. It has 286,011 nodes and 273,108 (mostly shell) elements. Kan et al. [10] used this model for frontal impact simulations and found the results to be consistent with physical crash test data. Fig. 2 shows the original FE model before and 100 ms after a frontal impact at 56.5 km/h.

Upon further examination of the original FE model, we found it to be unstable due to the existence of a significant amount of warped and highly skewed shell elements. When performing preliminary design simulations by changing the thickness of various parts, some of the simulation runs terminated with errors. In our initial attempt of sampling the design space, approximately one-third of 27 simulations crashed. Based on this observation, we modified and refined the model to improve its stability. The revised FE model has 320,998 nodes and 582,541 elements for approximately 1.8 million total degrees of freedom. Details about the revised Neon FE model can be found in Refs. [8,9]. The simulation and optimization results presented in this paper are all based on the revised FE model.

For crash simulations we used LS-DYNA v970 [22] on an IBM Linux Cluster with a total of 1038 1.266 GHz Pentium III processors and 607.5 GB RAM. A single simulation of 100 ms frontal impact (shown in Fig. 2) takes approximately ten hours using 36 processors.

We observed instabilities in our simulations using the explicit FE code, LS-DYNA, and had to adjust the numerical parameters for the input to complete some of the simulations. Similar problems were also reported and discussed in the literature by Brezzi and Bathe in their study of mixed FE formulations with details appearing in Refs. [23,24].

4.2. Design objectives and variables

The vehicle impact response is best described by the acceleration history with the peak acceleration typically

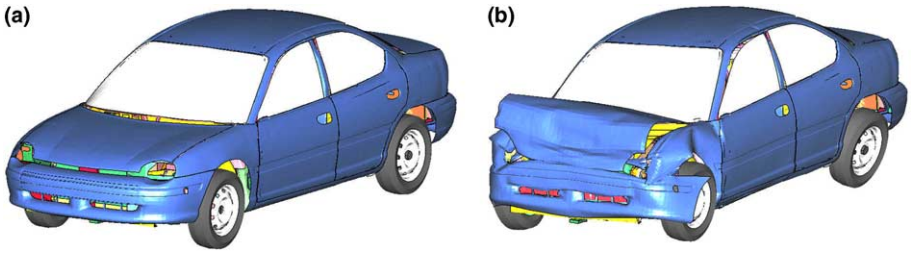

Fig. 2. Full-scale finite element model of 1996 Dodge Neon. (a) Before impact; (b) after 100 ms frontal impact.

used as a rough indicator of impact severity. The peak acceleration is determined by both the amount of kinetic energy that can be absorbed by the vehicle and the time that it takes for this energy to be absorbed. Therefore, there are two key factors to consider: energy absorption capacity and energy absorption rate. The goal of crashworthiness optimization is to maximize the vehicle's energy absorption capacity and rate in order to minimize the amount of energy transferred to the occupants.

Our preliminary vehicle frontal impact simulations showed that more than 40% of kinetic energy is absorbed within the first 20 ms and more than 90% within 40 ms. As indicated by the time history curves in Fig. 3, of 327 parts, thirteen are found to be responsible for 59% of the energy absorption at 20 ms and for 46% at 40 ms even though they make up only 3.7% of total vehicle mass. Consequently, we focused our attention on these thirteen parts with the FE model at the initial state and at three specific instances into the crash as shown in Fig. 4. It can also be observed from Fig. 4(c) and (d) that the amount of deformation from 40 to 100 ms is much less significant than that up to 40 ms. Therefore, the kinetic

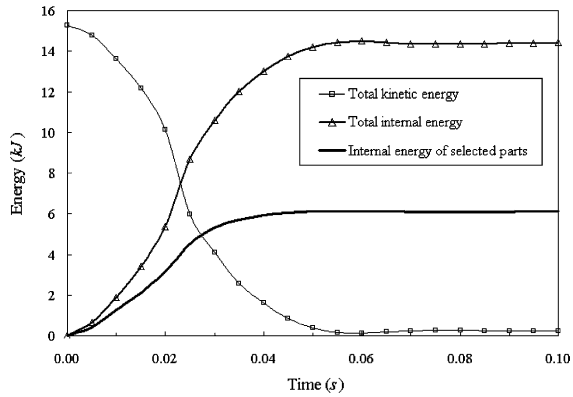

Fig. 3. Time history of total kinetic energy, total internal energy, and internal energy of thirteen selected parts.

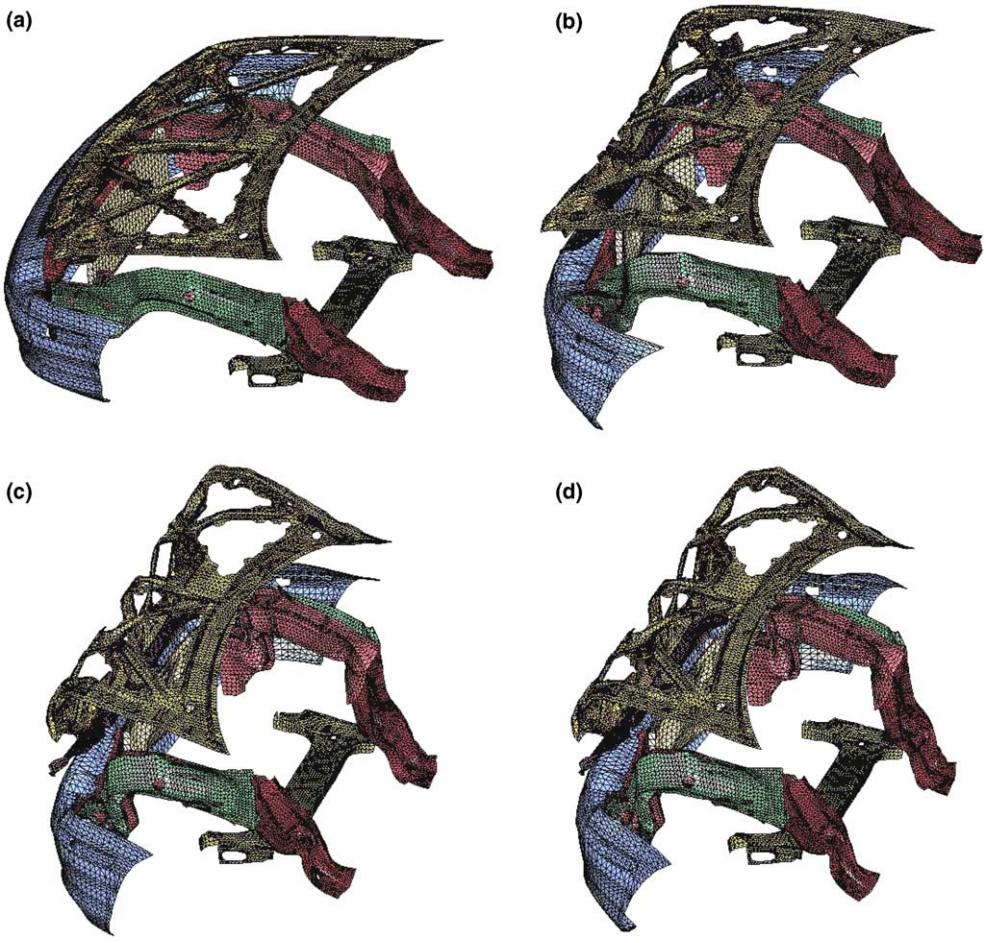

Fig. 4. FE model of thirteen selected parts at (a) initial state, (b) 20 ms, (c) 40 ms, and (d) 100 ms after impact.

energy absorbed by these thirteen parts at 20 ms and 40 ms were chosen as two objectives to be optimized.

Although we expected the peak acceleration to decrease as energy absorption capacity and rate are increased, their relationship, as will be discussed later, is not necessarily monotonic. Therefore, the peak acceleration measured at the engine top was selected as the third objective.

We chose part thickness as design variables. However, since among the selected parts three pairs are symmetric, only ten design variables are needed to describe the thickness of individual parts. Table 3 lists the thirteen parts along with the corresponding initial thickness, mass, and energy absorption at three different instances following the impact.

4.3. Optimization problem formulation

The multiobjective optimization problem described previously is formulated as

$$\begin{aligned} \text{Min} \quad & F(\boldsymbol{x}) = (-f_1(\boldsymbol{x}), -f_2(\boldsymbol{x}), f_3(\boldsymbol{x})) \\ \text{s.t.} \quad & \frac{M_{\text{new}}}{M_{\text{old}}} - 1 \leqslant 0 \\ & x_i^l \leqslant x_i \leqslant x_i^u \quad i = 1, \text{NDV}, \end{aligned} \tag{20}$$

where $f_1(\boldsymbol{x})$ and $f_2(\boldsymbol{x})$ represent the amount of energy absorbed (by the selected parts) at 20 ms and 40 ms, respectively, while $f_3(\boldsymbol{x})$ is the peak acceleration at engine top. The design constraint keeps the mass constant while the parts change thickness with M_{old} and M_{new} representing the mass of selected parts at the initial design and during optimization, respectively. Since objectives $f_1(\boldsymbol{x})$ and $f_2(\boldsymbol{x})$ are to be maximized, their negative forms are used in Eq. (20). The side constraints allow a ±50% variation in design variables from their initial values given in Table 3.

There are several alternative ways to convert a multiobjective optimization problem such as that defined by Eq. (20) into a single objective problem. In this study, we chose the weighted sum formulation with the revised optimization formulation expressed as

$$\begin{aligned} \text{Min} \quad & F(\boldsymbol{x}) = -W_1 f_1(\boldsymbol{x}) - W_2 f_2(\boldsymbol{x}) + W_3 f_3(\boldsymbol{x}) \\ \text{s.t.} \quad & \frac{M_{\text{new}}}{M_{\text{old}}} - 1 \leqslant 0 \\ & W_i 0, \sum W_i = 1, \quad i = 1, 3 \\ & x_i^l \leqslant x_i \leqslant x_i^u, \quad i = 1, NDV, \end{aligned} \tag{21}$$

where W_i represents the weight for the ith objective with the additional requirements that each weight has to be greater than zero and their sum cannot exceed one. By using different combinations of weight coefficients, a set of solutions is obtained and the Pareto non-dominance check is performed to obtain the Pareto Frontier. A well-known problem of the weighted sum method is that some of the solutions on the Pareto Frontier may be missing. However the purpose of this study is to compare model appropriateness instead of attempting to obtain the entire solution set; therefore, this method is appropriate for this study.

The optimization problem in Eq. (21) is solved using the object-oriented multidisciplinary optimization system developed at the Center for Advanced Vehicular Systems (CAVS), Mississippi State University [25]. This program uses the method of feasible sequential quadratic programming (FSQP) as the optimization solver [26]. Before optimization, we developed appropriate metamodels for the objective functions $f_1(\boldsymbol{x})$, $f_2(\boldsymbol{x})$, and $f_3(\boldsymbol{x})$ in Eq. (20) using RSM and RBF with the procedure described next.

4.4. Metamodeling with RSM and ANOVA analysis

With 10 design variables, a first-order RS model for each objective would consist of eleven unknown coefficients while a second-order model would have 21 unknown coefficients excluding the interaction terms. For

Table 3
Part thickness and response characteristic at initial design

Deign variable	Part no.	Thickness (mm)	Mass (kg)	Internal energy at 20 ms (kJ)	Internal energy at 40 ms (kJ)	Internal energy at 100 ms (kJ)
x_1	330	2.0	6.67	1.32	1.79	1.79
x_2	299	3.5	4.55	0.35	0.52	0.52
x_3	389 and 391	1.9	7.72	0.65	1.14	1.14
x_4	390 and 392	1.5	4.09	0.32	0.59	0.60
x_5	632	1.0	3.40	0.23	0.36	0.36
x_6	285	0.6	4.56	0.11	0.28	0.30
x_7	439	2.6	4.37	0.00	0.25	0.30
x_8	627	1.0	2.93	0.10	0.30	0.30
x_9	384	1.5	1.65	0.05	0.21	0.22
x_{10}	398 and 399	1.9	4.44	0.02	0.45	0.59
Total			44.37	3.16	5.92	6.11

the number of design variables involved, it would be impractical to use full factorial design (FFD) or central composite design (CCD) for calculation of the coefficients because the number of simulations required for these two methods would be too large. For example, a 2-level FFD would require $2^{10} = 1024$ simulations with CCD requiring an additional 21 simulations. However, the Taguchi L_{27} orthogonal array would require only 27 simulations for up to 13 design variables, each with three levels [27]. Thus, each design variable is allowed to have normalized values of -1, 0, 1 representing those at lower bound, initial design, and upper bound, respectively. Using the first ten columns in the L_{27} array as the design matrix, we performed 27 simulations and developed two separate (first- and second-order) RS models for each objective function. The design matrix and the normalized FEA results including those for the original structure are given in Table 4. The results of ANOVA for the first- and second-order RS models of each objective are shown in Table 5.

Both RS models for $f_1(\boldsymbol{x})$ have large F statistics at probability of less than 0.001. While the R^2 and R^2_{adj} of the second-order model are marginally better than those of the first-order model, both RS models have small

Table 4
Design matrix and normalized values of objective functions obtained from FE simulations

No.	x_1	x_2	x_3	x_4	x_5	x_6	x_7	x_8	x_9	x_{10}	$f_1(x)$	$f_2(x)$	$f_3(x)$
0	0	0	0	0	0	0	0	0	0	0	1.00	1.00	1.00
1	−1	−1	−1	−1	−1	−1	−1	−1	−1	−1	0.51	0.71	1.05
2	−1	−1	−1	−1	0	0	0	0	0	0	0.57	0.77	1.26
3	−1	−1	−1	−1	1	1	1	1	1	1	0.61	0.81	1.17
4	−1	0	0	0	−1	−1	−1	0	0	0	0.81	0.89	1.02
5	−1	0	0	0	0	0	0	1	1	1	0.87	0.92	0.94
6	−1	0	0	0	1	1	1	−1	−1	−1	0.87	0.88	0.78
7	−1	1	1	1	−1	−1	−1	1	1	1	1.05	1.00	0.95
8	−1	1	1	1	0	0	0	−1	−1	−1	1.00	0.94	0.80
9	−1	1	1	1	1	1	1	0	0	0	1.13	1.04	0.88
10	0	−1	0	1	−1	0	1	−1	0	1	1.00	1.01	0.93
11	0	−1	0	1	0	1	−1	0	1	−1	1.01	0.99	1.02
12	0	−1	0	1	1	−1	0	1	−1	0	1.11	1.06	0.75
13	0	0	1	−1	−1	0	1	0	1	−1	0.97	0.94	0.74
14	0	0	1	−1	0	1	−1	1	−1	0	1.04	1.02	1.04
15	0	0	1	−1	1	−1	0	−1	0	1	1.05	1.01	0.83
16	0	1	−1	0	−1	0	1	1	−1	0	0.81	0.92	1.16
17	0	1	−1	0	0	1	−1	−1	0	1	0.79	0.90	1.06
18	0	1	−1	0	1	−1	0	0	1	−1	0.79	0.87	1.08
19	1	−1	1	0	−1	1	0	−1	1	0	1.20	1.12	0.88
20	1	−1	1	0	0	−1	1	0	−1	1	1.23	1.13	0.67
21	1	−1	1	0	1	0	−1	1	0	−1	1.19	1.10	0.73
22	1	0	−1	1	−1	1	0	0	−1	1	0.98	1.03	0.80
23	1	0	−1	1	0	−1	1	1	0	−1	0.98	0.95	0.81
24	1	0	−1	1	1	0	−1	−1	1	0	1.00	1.02	0.91
25	1	1	0	−1	−1	1	0	1	0	−1	0.99	1.00	0.72
26	1	1	0	−1	0	−1	1	−1	1	0	0.96	1.01	0.87
27	1	1	0	−1	1	0	−1	0	−1	1	1.01	1.01	0.76

Table 5
Results of statistical analysis for first- and second-order RS models

Objective	RS model	F	$Pr > F$	R^2	R^2_{adj}	RMSE	PRESS	$R^2_{\text{prediction}}$
$f_1(\boldsymbol{x})$	First-order	99.9	<0.001	0.983	0.973	0.029	0.040	0.954
	Second-order	89.8	<0.001	0.996	0.985	0.022	0.056	0.935
$f_2(\boldsymbol{x})$	First-order	41.8	<0.001	0.961	0.938	0.025	0.028	0.894
	Second-order	112.6	<0.001	0.997	0.988	0.011	0.015	0.943
$f_3(\boldsymbol{x})$	First-order	3.5	0.0121	0.670	0.476	0.111	0.543	0.149
	Second-order	3.5	0.0472	0.910	0.651	0.091	1.084	0.0

RMSE. The model statistics indicate that both first- and second-order models for $f_1(\boldsymbol{x})$ fit sampling data very well, with the latter being slightly superior.

For $f_2(\boldsymbol{x})$ and $f_3(\boldsymbol{x})$, a similar ANOVA analysis was performed. The values of F, R^2, R^2_{adj}, and RMSE for $f_2(\boldsymbol{x})$ indicate that the second-order model is better than the first-order model. For $f_3(\boldsymbol{x})$, neither the first- nor the second-order model fits the data well. The first-order model has a small R^2 and R^2_{adj} and a relatively large RMSE (0.11) as compared to the rest. The second-order model is slightly better than the first; however, its relatively small R^2_{adj} and relatively large RMSE still indicate a poor fit.

The PRESS statistic and $R^2_{\text{prediction}}$ were also calculated for the metamodels of each objective function using Eqs. (11) and (12) with the results also given in Table 5. For $f_1(\boldsymbol{x})$ and $f_2(\boldsymbol{x})$, the large values of $R^2_{\text{prediction}}$ indicate that both first- and second-order RS models are fairly accurate with the second-order model in each case having a slight advantage. As for $f_3(\boldsymbol{x})$, the $R^2_{\text{prediction}}$ values of first- and second-order models are 0.149 and 0.0, respectively. These low values indicate that neither of the two RS models is a good predictor of the engine top acceleration response. The results of $R^2_{\text{prediction}}$ are consistent with those of ANOVA.

While mindful of the deficiencies of the RS model for $f_3(\boldsymbol{x})$, we proceeded to solve the optimization problem in Eq. (21) using a single global second-order RS model for each of the objective functions. The main intent was to generate random design points on the Pareto Frontier for subsequent comparison with the results from direct FE simulations as well as those based on more accurate metamodels.

As a single global model is created for each objective function, the model accuracy will be further checked and compared with the above prediction using off-design points obtained from FE validation results after optimization. Details are given in the next section.

4.5. Optimization using RS models

Due to the use of a gradient-based search technique, the optimization problem was solved starting from more than 100 random initial design points with the best solution chosen as the optimal design. A set of solutions can be obtained for this multiobjective optimization problem by repeating the above procedure with different combinations of the weight coefficients in Eq. (21). In this study, we used a minimum weight of 0.1 and a weight increment of 0.01. This means that the weight coefficients for $f_1(\boldsymbol{x})$, $f_2(\boldsymbol{x})$, and $f_3(\boldsymbol{x})$ are chosen from 0.1 to 0.8 satisfying the $\Sigma W_i = 1$ constraint. This approach resulted in 62,196 possible combinations and equal number of design solutions. The Pareto non-dominance criterion was then applied to the 62,196 solutions to obtain those on the Pareto Frontier. We used the predicted optimum designs at eight random points on the Pareto Frontier as identified in Table 6 for subsequent design validation using complete transient FE analysis to find the exact values of $f_1(\boldsymbol{x})$, $f_2(\boldsymbol{x})$, and $f_3(\boldsymbol{x})$ at each of the selected points. The exact values along with the predicted values of the three objectives are shown in Table 7.

For the eight selected points, we found the maximum and average errors in $f_1(\boldsymbol{x})$ to be 6.5% and 2.2%, respectively. For $f_2(\boldsymbol{x})$ the maximum and average errors are 3.2% and 1.5%, respectively. For $f_3(\boldsymbol{x})$, however, the results of the second-order RS model are rather poor, with the maximum error being 29.8% and average error 15.1%. Although it is possible to improve the RS model for $f_3(\boldsymbol{x})$, it would require additional simulation runs. An alternative approach would be to develop RBF-based solutions using the same number of response samples as in the case of RSM. This procedure is discussed next.

4.6. Evaluation of RSM-based results with RBF

To investigate whether RBF-based metamodels are any better than the RS models, we selected five types of RBF and developed a model for each objective function. The five RBFs are:

(a) Gaussian with linear polynomial;
(b) Multiquadric with linear polynomial;
(c) Inverse-multiquadric with linear polynomial;
(d) Multiquadric;
(e) Inverse-multiquadric.

Table 6
Design variables at eight optimum points based on second-order RS models

Design point	x_1	x_2	x_3	x_4	x_5	x_6	x_7	x_8	x_9	x_{10}
1	1.00	−1.00	1.00	1.00	0.90	−1.00	−1.00	−1.00	−1.00	−0.78
2	1.00	−1.00	1.00	1.00	−1.00	−1.00	−0.56	−1.00	−1.00	0.24
3	1.00	−0.03	0.58	1.00	−1.00	−1.00	0.42	−1.00	−1.00	−1.00
4	1.00	−0.99	1.00	1.00	−1.00	−1.00	−0.41	−1.00	−1.00	0.08
5	1.00	−0.68	1.00	1.00	−1.00	−1.00	−0.44	−1.00	−1.00	−0.20
6	1.00	−0.82	0.96	1.00	1.00	−1.00	−0.97	−1.00	−1.00	−1.00
7	1.00	−0.98	0.96	1.00	1.00	−1.00	−0.81	−1.00	−1.00	−1.00
8	1.00	−0.26	1.00	1.00	−1.00	−1.00	−0.07	−1.00	−1.00	−1.00

Table 7
Comparison of RSM predicted optima with FEA simulation results

Design point	$f_1(x)$ (kJ)			$f_2(x)$ (kJ)			$f_3(x)$ (m/s^2)		
	RSM	FEA	% Error	RSM	FEA	% Error	RSM	FEA	% Error
1	4.01	4.04	0.8	6.64	6.73	1.2	−1349.4	−1515.6	11.0
2	3.98	4.05	1.8	6.82	6.98	2.2	−1507.0	−1532.4	1.7
3	3.78	3.66	3.1	6.36	6.28	1.4	−1046.9	−1492.2	29.8
4	3.98	4.06	1.9	6.81	6.93	1.7	−1490.7	−1477.1	0.9
5	3.99	4.05	1.6	6.75	6.89	1.9	−1407.7	−1592.2	11.6
6	3.99	3.95	0.9	6.55	6.59	0.6	−1188.4	−1505.5	21.1
7	3.98	3.93	1.3	6.57	6.57	0.1	−1201.4	−1445.3	16.9
8	3.93	3.69	6.5	6.48	6.28	3.2	−1089.3	−1515.3	28.1
Ave.			2.2			1.5			15.1
Max.			6.5			3.2			29.8

Functions (a)–(c) are augmented RBFs in the format given by Eq. (16). The augmented RBFs are more desirable than the regular RBFs, because the formers can handle linear responses in addition to nonlinear ones. However, the results in Table 2 show that the augmented RBF created with the multiquadric and inverse-multiquadric functions are slightly worse than the corresponding non-augmented models. Therefore, we also examine the non-augmented RBF models created with the two functions as given in (d) and (e). The augment RBF model created with the Gaussian function is better than the non-augmented one in Table 2; therefore, we use the augment RBF format in this problem as given in (a).

On the right hand side of Eq. (16) there are 28 unknown coefficients in the first term corresponding to the 28 design points (one from original structure and 27 from Taguchi array). The second term is a linear polynomial that has 11 unknown coefficients (one being the constant and the others for the 10 design variables). These 39 unknown coefficients are solved by Eq. (18), which also includes the orthogonality condition given by Eq. (17). Functions (d) and (e) follow the format given by Eq. (13), and the 28 unknown coefficients are solved by Eq. (15). Hence, in all functions only 28 observations are used to solve for the unknown coefficients.

Using the RBF-based models, we evaluated the objective functions at the eight design points given in Table 6 with a summary of results shown in Figs. 5–7. Also included in the same figures are the objective function values from RSM-based solutions and direct FE simulations. It can be seen from Figs. 5 and 6 that the predicted values for $f_1(x)$ and $f_2(x)$ by Function (e) are poor and significantly different from those by Functions

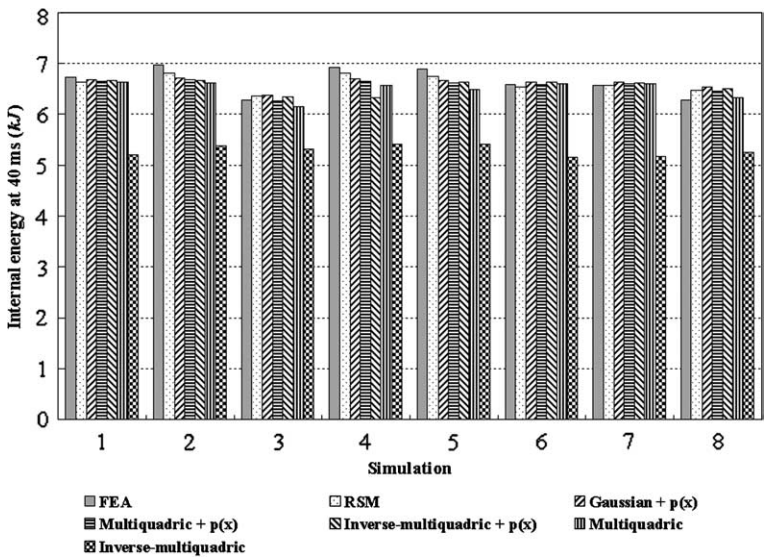

Fig. 5. Comparison of metamodels and FEA results for $f_1(x)$.

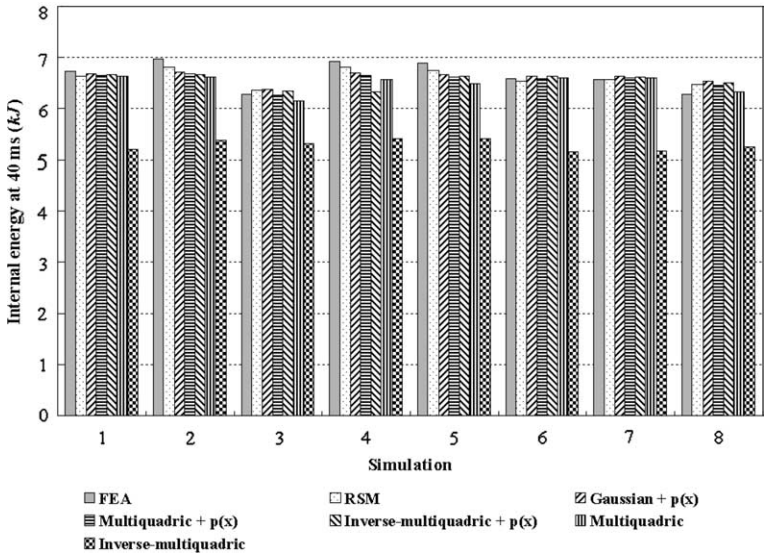

Fig. 6. Comparison of metamodels and FEA results for $f_2(\boldsymbol{x})$.

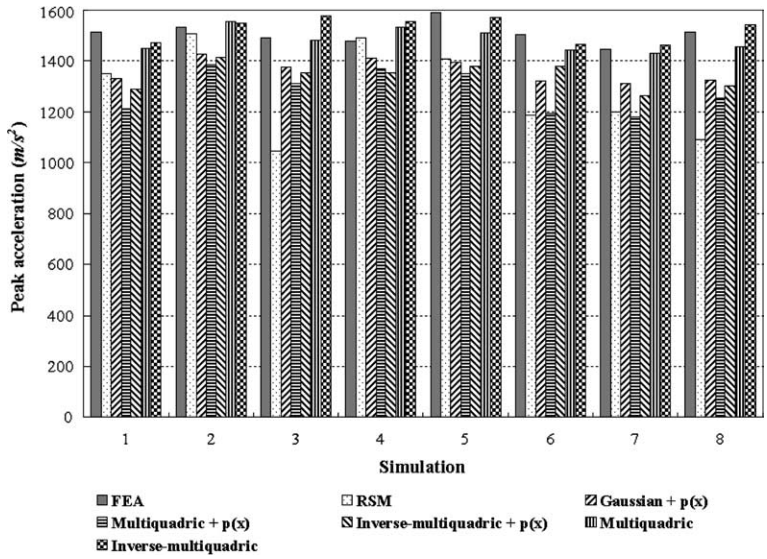

Fig. 7. Comparison of metamodels and FEA results for $f_3(\boldsymbol{x})$.

(a)–(d). Fig. 6 shows that Functions (d) and (e) give better overall predictions than Functions (a)–(c).

The errors of predicted values by the five RBFs compared to the true values obtained directly from FE simulations are given in Table 8. For $f_1(\boldsymbol{x})$, the maximum errors of Functions (a)–(e) are 6.7%, 4.4%, 8.5%, 8.1%, and 28.7%, while the average errors are 2.6%, 2.2%, 3%, 4.7%, and 26%, respectively. This shows that Functions (a)–(d) give reasonably good predictions of the true response while Function (e) does not. A similar trend is seen for $f_2(\boldsymbol{x})$ as well. The maximum errors of the five RBFs for $f_2(\boldsymbol{x})$ are 4.3%, 4.2%, 8.5%, 5.8%, and 28.7%, with average errors being 2.3%, 2.1%, 3%, 2.6%, and 26%, respectively. For $f_3(\boldsymbol{x})$, Functions (a)–(c) give poor predicted values while Functions (d) and (e) give good predictions. The maximum errors of the five RBFs for $f_3(\boldsymbol{x})$ are 12.5%, 20.8%, 15%, 5.1%, and 5.8%, while the average errors are 9.7%, 15%, 11%, 3%, and 2.7%, respectively.

The analyses in Sections 4.4 and 4.5 showed that the global, second-order RS model (based on 28 observations) cannot suitably represent $f_3(\boldsymbol{x})$, which appears to

Table 8
Percentage errors of RBF predicted optima compared to FEA simulation results

Objective	Design point	Gaussian + polynomial	Multiquadric + polynomial	Inv-multiquadric + polynomial	Multiquadric	Inverse multiquadric
$f_1(\boldsymbol{x})$	1	0.5	0.9	0.0	4.6	28.7
	2	2.1	3.2	2.5	6.8	27.4
	3	2.2	0.1	1.4	4.3	21.2
	4	2.3	3.5	8.5	7.2	26.9
	5	2.4	3.7	2.9	8.1	26.7
	6	2.2	0.6	0.4	3.2	27.8
	7	2.7	1.3	2.2	2.5	27.2
	8	6.7	4.4	5.8	0.8	21.8
	Ave.	2.6	2.2	3.0	4.7	26.0
	Max.	6.7	4.4	8.5	8.1	28.7
$f_2(\boldsymbol{x})$	1	0.7	1.2	0.9	1.4	22.6
	2	3.6	4.2	4.4	5.3	23.0
	3	1.6	0.1	1.0	1.8	15.5
	4	3.3	3.9	8.5	5.1	21.9
	5	3.3	4.0	3.6	5.8	21.3
	6	0.7	0.0	0.7	0.1	21.6
	7	1.1	0.5	0.9	0.5	21.2
	8	4.3	2.7	3.7	0.9	16.2
	Ave.	2.3	2.1	3.0	2.6	20.4
	Max.	4.3	4.2	8.5	5.8	23.0
$f_3(\boldsymbol{x})$	1	12.1	20.0	15.0	4.2	2.9
	2	6.8	9.4	7.7	1.4	1.1
	3	7.7	12.0	9.1	0.7	5.8
	4	4.4	7.1	8.2	3.9	5.2
	5	12.4	15.2	13.4	5.1	1.3
	6	12.2	20.8	8.4	4.1	2.5
	7	9.1	18.3	12.4	0.9	1.2
	8	12.5	17.2	14.1	3.8	1.9
	Ave.	9.7	15.0	11.0	3.0	2.7
	Max.	12.5	20.8	15.0	5.1	5.8

be a highly nonlinear function within the entire design space. The models created by RBFs (a)–(c), with all augmented by a linear polynomial as shown in Eq. (20), also did poorly when it comes to $f_3(\boldsymbol{x})$. On the other hand, the models created by Functions (d) and (e), which do not include polynomial terms, give better predictions of $f_3(\boldsymbol{x})$. The poor predictability of models in Functions (a)–(c) may in fact be caused by the extra constraints (i.e., the orthogonality condition) when trying to solve 39 unknown coefficients with only 28 observations. This suggests that RBFs without polynomial terms may be better suited for approximating highly nonlinear functions when the sample size is relatively small.

Among the five RBFs, Function (d), the multiquadric function without polynomials, is identified to be the most stable function for all three objectives. Therefore, the models created by the multiquadric function were selected to perform the multiobjective optimization again with the results presented in the next section.

4.7. Optimization results using multiquadric RBF

The optimization problem in Eq. (21) was solved using different combination of weight coefficients for $f_1(\boldsymbol{x})$, $f_2(\boldsymbol{x})$, and $f_3(\boldsymbol{x})$. The procedure for obtaining solutions on the Pareto Frontier is the same as that described previously in Section 4.5. The design variables at eight randomly selected optimum points on the Pareto Frontier are shown in Table 9 with the estimated and exact values of the three objectives at these points given in Table 10. The maximum errors of the RBF models for $f_1(\boldsymbol{x})$, $f_2(\boldsymbol{x})$, and $f_3(\boldsymbol{x})$ are 5.4%, 5.2%, and 7.2% while the average errors are 2.2%, 2%, and 5.7%, respectively.

Table 9
Design variables at eight optimum points based on multiquadric RBF models

Design point	x_1	x_2	x_3	x_4	x_5	x_6	x_7	x_8	x_9	x_{10}
1	1.00	−1.00	1.00	1.00	0.90	−1.00	−1.00	−1.00	−1.00	−0.78
2	1.00	−1.00	1.00	1.00	−1.00	−1.00	−0.56	−1.00	−1.00	0.24
3	1.00	−0.03	0.58	1.00	−1.00	−1.00	0.42	−1.00	−1.00	−1.00
4	1.00	−0.99	1.00	1.00	−1.00	−1.00	−0.41	−1.00	−1.00	0.08
5	1.00	−0.68	1.00	1.00	−1.00	−1.00	−0.44	−1.00	−1.00	−0.20
6	1.00	−0.82	0.96	1.00	1.00	−1.00	−0.97	−1.00	−1.00	−1.00
7	1.00	−0.98	0.96	1.00	1.00	−1.00	−0.81	−1.00	−1.00	−1.00
8	1.00	−0.26	1.00	1.00	−1.00	−1.00	−0.07	−1.00	−1.00	−1.00

Table 10
Comparison of RBF predicted optima with FEA simulation results

Design point	$f_1(\boldsymbol{x})$ (kJ)			$f_2(\boldsymbol{x})$ (kJ)			$f_3(\boldsymbol{x})$ (m/s^2)		
	RBF	FEA	% Error	RBF	FEA	% Error	RBF	FEA	% Error
1	3.86	3.92	1.5	6.63	6.54	1.4	−1441.4	−1551.4	7.1
2	3.86	4.00	3.5	6.64	6.67	0.4	−1451.8	−1534.3	5.4
3	3.85	3.90	1.3	6.62	6.56	0.9	−1434.9	−1467.3	2.2
4	3.85	3.91	1.4	6.61	6.57	0.6	−1430.8	−1532.0	6.6
5	3.85	3.65	5.4	6.65	6.33	5.2	−1522.2	−1627.7	6.5
6	3.85	3.89	1.1	6.60	6.50	1.6	−1428.8	−1539.4	7.2
7	3.84	3.73	3.1	6.66	6.40	4.1	−1544.5	−1619.0	4.6
8	3.84	3.83	0.3	6.68	6.59	1.4	−1570.1	−1672.3	6.1
Ave.			2.2			2.0			5.7
Max.			5.4			5.2			7.1

Although RBF based solutions are superior to those based on RSM, there are clear drawbacks. It should be noted that a metalmodel created by RBF consists of the same number of basis functions as response samples; therefore an RBF model is computationally more expensive than an RS model. For multiobjective optimization problems the computational cost becomes significant in that a large number of function evaluation is needed to assess the entire Pareto Frontier. Another disadvantage of RBF is that model predictability at the selected sampling points cannot be determined using ANOVA, because by definition an RBF model passes through all the design points. Thus, it can be difficult to select the best RBF before the models are used in design optimization since the best RBF may be problem dependant and can only be found through validation at off-design points.

We select the results of the third FE simulation in Table 10 to illustrate the improvements on the vehicle design through optimization. The true values of the

Table 11
Part thickness and response characteristics at optimal design based on multiquadric RBF models

Deign variable	Part no.	Thickness (mm)	Mass (kg)	Internal energy at 20 ms (kJ)	Internal energy at 40 ms (kJ)	Internal energy at 100 ms (kJ)
x_1	330	2.9	10.00	1.99	2.51	2.50
x_2	299	1.8	2.28	0.21	0.44	0.46
x_3	389 and 391	2.8	11.57	0.57	1.10	1.13
x_4	390 and 392	2.3	6.13	0.29	0.55	0.58
x_5	632	1.4	4.91	0.40	0.60	0.61
x_6	285	0.3	2.28	0.07	0.18	0.21
x_7	439	1.3	2.18	0.08	0.35	0.45
x_8	627	0.7	1.96	0.08	0.18	0.19
x_9	384	0.8	0.83	0.06	0.19	0.21
x_{10}	398 and 399	0.9	2.22	0.17	0.45	0.60
Total			44.37	3.90	6.56	6.92

Table 12
Comparison of initial (baseline) and optimal designs

Item	Before optimization	After optimization	% Change
Total weight of selected parts (kg)	44.37	44.37	0.0
Internal energy at 20 ms (kJ)	3.16	3.90	23.4
Internal energy at 40 ms (kJ)	5.92	6.56	10.8
Internal energy at 100 ms (kJ)	6.11	6.92	13.3
Peak acceleration (m/s^2)	−2126.0	−1467.3	−31.0

ten design variables, i.e., the thickness of thirteen selected parts, are calculated using the original values in Table 3 and the normalized values in the third row of Table 9. The internal energies of the optimized parts at 20 ms, 40 ms, and 100 ms are given in Table 11 along with each part thickness. A comparison of the initial and optimum designs with respect to mass, internal energy absorption, and the peak acceleration is shown in Table 12. Fig. 8 illustrates the time histories of the total internal energy of the thirteen parts before and after optimization. Fig. 9 shows a comparison of acceleration histories for both the original and optimum designs. The optimum design has an increased energy absorption capacity at all measured instances and decreased peak acceleration without any increase in the total vehicle mass. The energy absorbed by the thirteen parts are 23.4%, 10.8%, and 13.3% more than those of the original design at 20 ms, 40 ms, and 100 ms, respectively. The peak acceleration of the optimum design is reduced by 31% over the original design. These results show that a significant improvement in vehicle's crashworthiness performance can be made without incurring mass penalty, a key factor affecting the manufacturing cost.

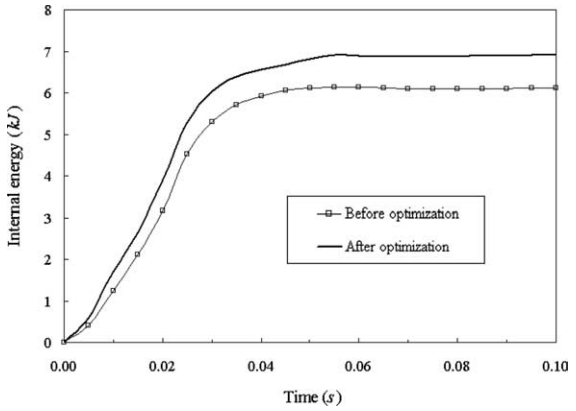

Fig. 8. Time history of internal energy for selected parts before and after optimization.

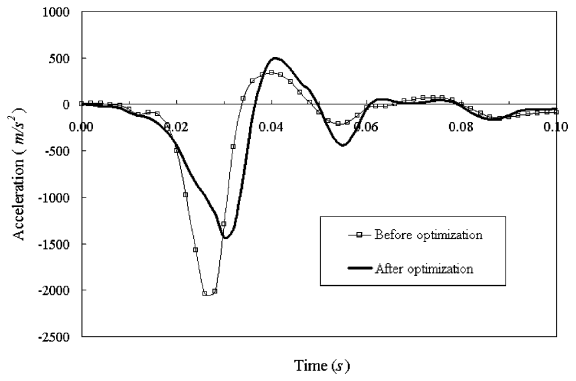

Fig. 9. Peak acceleration measured at the engine top before and after optimization.

5. Conclusions

In this paper, we discussed the development, application, and accuracy of RSM and RBF based metamodels in multiobjective crashworthiness optimization of a full-scale vehicle model. Because of the high computational simulation cost, metamodels were developed using a relatively small number of simulation samples. Among the three design objectives considered, the engine top acceleration was the most difficult to model due to its highly nonlinear relationship with the selected design variables. Although both first- and second-order RS models produced acceptable estimates for energy absorption responses, they failed to produce good results for the engine top acceleration. By contrast, multiquadric and inverse-multiquadric RBFs resulted in fairly accurate response models even for engine top acceleration. In particular, the multiquadric function was found to produce the most stable RBF for all three objective functions. This is consistent with the founding in the accuracy assessment of metamodels created for the nonlinear Branin rcos function.

The use of RSM or RBF, especially in a complex problem such the one considered in this paper, involves several tradeoffs that could ultimately be traced to the need for additional response samples. In the case of RSM, the inclusion of interaction terms (in the second-order model) does require additional response samples whereas the examination of model accuracy through ANOVA does not. Similarly, in the case of RBF, the inclusion of augmenting polynomials was

unnecessary but in order to check the accuracy of an RBF model, it was necessary to conduct additional simulations, as ANOVA could not be used.

Finally, the successful implementation of a multiobjective optimization scheme showed that vehicle performance could be improved without an increase in vehicle mass, which is a major consideration in design and manufacturing of automobile bodies.

Acknowledgement

The authors acknowledge support of the Center for Advanced Vehicular Systems (CAVS), Mississippi State University.

References

[1] National Highway Traffic Safety Administration (NHTSA) Report: 2002 annual assessment motor vehicle traffic crash fatality and injury estimates for 2002. NCSA, 2003.
[2] Federal Motor Vehicle Safety Standards and Regulations. US Department of Transportation, National Highway Traffic Safety Administration. Washington, DC: 1998.
[3] Marklund PO, Nilsson L. Optimization of a car body component subjected to side impact. Struct Multidiscip Optim 2001;21:383–92.
[4] Kim CH, Mijar AR, Arora JS. Development of simplified models for design and optimization of automotive structures for crashworthiness. Struct Multidiscip Optim 2001;22:307–21.
[5] Redhe M, Forsberg J, Jansson T, Marklund PO, Nilsson L. Using the response surface methodology and the D-optimality criterion in crashworthiness related problems. Struct Multidiscip Optim 2002;24:185–94.
[6] Avalle M, Chiandussi G, Belingardi G. Design optimization by response surface methodology: application to crashworthiness design of vehicle structures. Struct Multidiscip Optim 2002;24:325–32.
[7] Kirkpatrick SW, Simons JW, Antoun TH. Development and validation of high fidelity vehicle crash simulation models. Int J Crash 1999;4:395–405.
[8] Zaouk AK, Marzougui D, Bedewi NE. Development of a detailed vehicle finite element model. Part I: Methodology. Int J Crash 2000;5:25–35.
[9] Zaouk AK, Marzougui D, Kan CD. Development of a detailed vehicle finite element model. Part II: Material characterization and component testing. Int J Crash 2000; 5:37–50.
[10] Kan CD, Marzougui D, Bahouth GT, Bedewi NE. Crashworthiness evaluation using integrated vehicle and occupant finite element models. Int J Crash 2001;6.
[11] Alexandrov NM, Dennis JE, Lewis RM, Torczon V. A trust region framework for managing the use of approximation models in optimization. Struct Multidiscip Optim 1998;15:16–23.
[12] Rais-Rohani M, Singh MN. Comparison of global and local response surface techniques in reliability-based optimization of composite structures. Struct Multidiscip Optim 2003;26:333–45.
[13] Wang G, Dong Z, Aitchison P. Adaptive response surface method—a global optimization scheme for approximation-based design problems. J Eng Optim 2001;33:707–34.
[14] Rodriguez J, Renaud JE, Watson LT. Trust region augmented Lagrangian methods for sequential response surface approximation and optimization. In: Proceedings of DETC'97 ASME design engineering technical conference. Sacramento, CA: Paper no. DETC97/DAC3773, ASME, 1997.
[15] Yang BS, Yeun YS, Ruy WS. Managing approximation models in multi-objective optimization. Struct Multidiscip Optim 2002;24:141–56.
[16] Jin R, Chen W, Simpson TW. Comparative studies of metamodelling techniques under multiple modeling criteria. Struct Multidiscip Optim 2001;23:1–13.
[17] Krishnamurthy T. Response surface approximation with augmented and compactly supported radial basis functions. The 44th AIAA/ASME/ASCE/AHS/ASC structures, structural dynamics, and materials conference. Norfolk, VA: 2003.
[18] Daberkow DD, Mavris DN. An investigation of metamodelling techniques for complex systems design. The 9th AIAA/ISSMO symposium on multidisciplinary analysis and optimization. Atlanta, GA: 2002.
[19] Montgomery DC. Design and analysis of experiments. 5th ed. New York: John Wiley & Sons; 2001.
[20] Hardy RL. Multiquadratic equations of topography and other irregular surfaces. J Geophys 1971;76:1905–15.
[21] Branin FK. A widely convergent method for finding multiple solutions of simultaneous nonlinear equations. IBM J Res Develop 1972;16:504–22.
[22] LS-DYNA Keyword User's Manual, version 970. Livermore Software Technology Corporation, 2003.
[23] Brezzi F, Bathe KJ. A discourse on the stability conditions for mixed finite element formulations. Comput Meth Appl Mech Eng 1990;82:27–57.
[24] Bathe KJ. The inf–sup condition and its evaluation for mixed finite element methods. Comput Struct 2001;79: 243–52.
[25] Fang H, Horstemeyer MF. An integrated design optimization framework using object-oriented programming. In: Proceedings of the 10th AIAA/ISSMO multidisciplinary analysis and optimization conference. Albany, NY: 2004. Paper no. AIAA-2004-4499.
[26] Lawrence CT, Zhou JL, Tits AL. User's guide for CFSQP, Ver2.5. Electrical Engineering Department and Institute for Systems Research, University of Maryland, College Park, MD, 1997.
[27] Taguchi G. Taguchi method—design of experiments. Quality engineering series, vol. 4. Tokyo: Japanese Standards Association, ASI Press; 1993.